Geo-Marine Letters, Vol.28(1); 15-22p.

Depth anomalies in the Arabian Basin, NW Indian Ocean

K.K. Ajay* **& A.K. Chaubey***

* National Institute of Oceanography, Dona Paula, Goa 403004, India

Abstract

We present previously unreported depth anomalies in the Arabian Basin, northwest Indian Ocean, to provide constraints on the evolution of the oceanic lithosphere of that basin. The depth anomaly reported in this study was calculated as the difference between the observed depth to oceanic basement (corrected for sediment load) and the calculated depth to oceanic basement of the same age. The results indicate an anomalous depth to basement of oceanic crust in the Arabian Basin in the age bracket of 63–42 Ma, suggesting that subsidence in this basin does not follow the age–depth relationship of normal oceanic crust. The depth anomalies in the basin vary from +501 to –905 m. A negative depth anomaly zone, mapped in the eastern part of the basin near the Laccadive Ridge, indicates that here the basement depth is shallower than predicted. By contrast, a positive depth anomaly zone, mapped in the western part of the basin, indicates a deeper basement depth than expected.

We propose that the excess subsidence of basement of the western part of the basin is probably caused by a relatively cold mantle, compared to the nearby eastern part of the basin which is affected by the intense thermal field of the former Reunion hotspot. Here, the rise in oceanic basement is caused by the vertical upwelling of oceanic crust due to convection, followed by a lateral across-axis flow facilitated by the Reunion hotspot at the time of spreading in early Tertiary times. This interpretation is in good agreement with spreading-ridge propagation and ridge–hotspot interaction reported earlier for the basin.

==========

Corresponding author : K.K. Ajay

e**-mail:** kajay@nio.org

Introduction

The Arabian Basin is bounded to the northwest by the Owen Fracture Zone which demarcates the transform boundary between the Indian and Arabian plates. The uneven topography of the NW-SE-trending active Carlsberg Ridge, which separates the Indian and African plates, forms the south-western boundary, whereas most of the north-eastern and eastern limits of the basin are bounded by the aseismic Laxmi and Laccadive ridges (Fig. 1). The basin is covered by Indus Fan sediments, which also determine the submarine topography. The water depth in this area varies from 3,400 m in the north to about 4,400 m in the south, the relatively smooth, sediment-covered seafloor generally dipping southwards. The sediment in this basin is of variable thickness, ranging from 1.3 to 4.2 km with velocity variations from 1.7 to 3.8 km/s (Naini and Talwani 1983). The oceanic crustal layers 2 and 3 underlying the sediments have average velocities of 5.51 and 6.67 km/s respectively.

The evolutionary history of the Arabian and Eastern Somali basins suggests that they are conjugate ocean basins created by seafloor spreading along the Carlsberg Ridge during the early Tertiary (McKenzie and Sclater 1971; Whitmarsh 1974; Norton and Sclater 1979; Naini and Talwani 1983; Bhattacharya et al. 1992; Chaubey et al. 1993, 1995; Mercuriev et al. 1995). More recent studies (Miles and Roest 1993; Dyment 1998; Chaubey et al. 1998, 2002) revealed that the evolution of these basins was dominated by a complex pattern of spreading-ridge propagation between 63 and 42 Ma. The successive spreading-ridge propagation resulted in an asymmetrical crustal accretion in the Arabian and Eastern Somali basins.

During the evolution of the basins, two major geodynamic events took place: the onset of Reunion hotspot activity (Deccan volcanics) and the Indo-Eurasian continental collision. The Deccan trap eruption, an apparently rapid event at chron 29r (~65 Ma; Courtillot et al. 1986; Vandamme et al. 1991; Bhattacharji et al. 1996), may have triggered the opening of the Carlsberg Ridge. Subsequently, the Reunion hotspot interacted with the northward-moving Indian plate and built the northern part of the Chagos-Laccadive Ridge on the rifted continental crust of India. The Indo-Eurasian continental collision, which started at about chron 24n (52 Ma; Patriat and Achache 1984), continues up to today. The evolution of the two basins may thus have been dominated by these two major geodynamic events due to their overriding regional influence.

The major objective of this study is to document previously unreported basement depth anomalies in the Arabian Basin, which is considered to have a normal oceanic crust. Based on an analysis of the depth anomaly, we discuss the impact of the former Reunion hotspot with the evolving young ocean crust of the basin during the early Tertiary.

Materials and methods

This study is based on published seismic refraction data (Naini and Talwani 1983), the results of the Deep Sea Drilling Project (DSDP) for sites 220–221 (Whitmarsh et al. 1974), and the regional magnetic isochron map of Chaubey et al. (2002). Locations of refraction stations, DSDP sites and magnetic isochron coverage are shown in Fig. 1 (note that all figures were drafted with GMT Software; Wessel and Smith 1995). Oceanic basement in the study area is identified by considering 5.51 km/s as the representative interval velocity of oceanic crustal layer 2 underlying the sediments. For a start, depth to oceanic basement and sediment thickness overlying the oceanic crust at each refraction station were calculated. Thereafter, the basement age at a particular location was obtained by using the magnetic isochron map (Chaubey et al. 2002) and the geomagnetic polarity reversal timescale (Cande and Kent 1995).

We use the term 'basement depth anomaly' (Menard 1973) to define the difference between the present depth of oceanic crust of known age (corrected for sediment load) and the predicted depth of the oceanic crust of the same age. We also apply the convention of describing negative and positive basement depth anomalies as the rise and excess subsidence of the present basement respectively, relative to the predicted basement.

According to the theory of plate tectonics, new oceanic lithosphere accreted at spreading ridges cools and contracts uniformly as it moves away from the spreading ridges. The change in depth to seafloor from the ridge crest to the ocean basin is a unique function of crustal age (Menard 1969), and is caused by cooling and thickening of oceanic lithosphere. The resulting correlation of ocean depth with crustal age (Menard 1969, 1973; Sclater and Francheteau 1970; Davis and Lister 1974; Parsons and Sclater 1977; McKenzie et al. 1980; Hayes 1988; Stein and Abbott 1991; Stein and Stein 1992; Hillier and Watts 2004; Louden et al. 2004) has been used as a powerful tool in understanding the tectonic history of oceanic plates. However, there are some areas in the oceans which do not follow the generally accepted empirical age–depth relation. The Arabian Basin is one such region. In this study, theoretical

basement depths have been calculated using the lithospheric thermal model for global depth and heat-flow (GDH1) of Stein and Stein (1992), derived for the crust older than 20 Ma. The theoretical basement depth $D(t)$ at a given ocean floor of age t Ma ($t \geq 20$ Ma) is given as:

$$D(t) = 5,651 - 2,473\exp(-0.0278t) \qquad (1)$$

The age of the oceanic basement was obtained using the regional magnetic isochron map (Chaubey et al. 2002) and the geomagnetic reversal timescale (Cande and Kent 1995). The age of the oceanic basement in the Arabian Basin varies from ~62.5 Ma (anomaly 28ny) in the northern part to ~38.4 Ma (anomaly 18ny) in the southern part. We calculated the age of the oceanic basement at each refraction station by linear interpolation using the half-spreading rate and the identified magnetic lineation pattern. Some of the refraction stations have not been considered as they are located in transferred crust regions for which the crustal age determination would not be accurate. Theoretical basement depths were then calculated from the estimated age and age–depth empirical Eq. (1).

We corrected observed basement depth by removing the sediment load. The corrections for the isostatic compensation of sediment load (ΔS) overlying the basement at each seismic refraction station was computed using the following formula (Crough 1983):

$$\Delta S = d(\rho_a - \rho_s)/(\rho_a - \rho_w) \qquad (2)$$

where ρ_a=3.3 gm/cm^3 and ρ_W=1.03 gm/cm^3 are the densities of the upper mantle and seawater respectively, and ρ_S and d are the density and thickness respectively of the sediment above the basement. The corrected depth to basement (D_c) was then calculated using the following formula (Hayes 1988):

$$D_c = d_w + \Delta S \qquad (3)$$

where d_W is observed water depth. The Nafe-Drake velocity–density relationship (Nafe and Drake 1963) was used to compute the density of the sedimentary column. The average seismic velocity (V_a) of a multi-layer sedimentary column was computed using the following formula:

$$V_a = (e_1 + e_2 + ... + e_n)/(e_1/v_1 + e_2/v_2 + ... + e_n/v_n) \qquad (4)$$

where e_1, e_2, … e_n and v_1, v_2, … v_n are the thicknesses and interval velocities of the sedimentary layers 1, 2, … n respectively, as obtained from the seismic refraction data.

By subtracting basement depth predicted by the GDH1 model from sediment-corrected basement depth, we computed the basement depth anomaly of the study area, as presented in

Table 1. The depth anomalies obtained after removal of the lithospheric cooling effect can be interpreted in terms of crustal and upper mantle sources and flexure of the lithosphere.

Results

Depth variations in the Arabian Basin indicate the presence of both positive and negative anomalies which vary from 501 to –905 m (Table 1). These anomalies, observed over 63–42 Ma old oceanic crust of the basin, are not distributed randomly but rather show a distinct pattern – a zone of negative anomalies, followed by a zone of positive anomalies. The negative depth anomaly zone, which signifies a rise of oceanic basement, is located towards the eastern part of the Arabian Basin, immediately west of the Laccadive Ridge. The positive depth anomaly zone, by contrast, signifies excess subsidence and lies in the western part of the Arabian Basin (Fig. 2).

Large (>300 m) positive depth anomalies (deeper basement than predicted) are observed at locations 64V34, 66V34, 67C17 and 68C17 in the positive depth anomaly zone (Figs. 1, 2). These locations show excess subsidence and coincide with the sediment depocentre of the Arabian Basin. The depocentre region, which is located between about 64º and 67ºE and 14º and 17ºN, approximately corresponds to the centre of the Indus Cone where over 3 km of sediment has accumulated (Naini 1980).

In the negative depth anomaly zone (shallower basement than predicted), the negative depth anomalies increase from west to east towards the Laccadive Ridge, even though the basement age increases in the same direction. This indicates that the corrected basement depth becomes shallower towards the Laccadive Ridge, and does not follow the depth predicted by the thermal cooling and thickening of normal oceanic lithosphere in this part of the Arabian Basin. As we discuss below, the shoaling of the basement is related to the Reunion hotspot which was active during the early Tertiary, when it interacted with the northward-moving Indian plate to build the Laccadive Ridge on the rifted continental crust of India.

We have presented two profiles (Figs. 2, 3) across the Arabian Basin, showing observed basement depths, basement depths obtained after sediment load correction, and basement depths predicted by the lithospheric thermal model GDH1 of Stein and Stein (1992). These profiles pass from southwest to northeast, and traverse from positive to negative depth anomaly zones. It may be noted that even though the age of the oceanic crust along the profile progressively increases towards the northeast, basement depths (corrected for sediment load) do not follow the predicted trend but rather show two well-defined patterns.

Profile 1 shows low-amplitude positive depth anomalies (deeper basement than predicted), followed by a systematic increase in negative depth anomalies (shallower basement than predicted) towards the northeast. Profile 2, by contrast, shows a general increase in positive depth anomalies, implying deeper basement than predicted by the thermal cooling model. This deepening of the basement attains its maximum value in the sediment depocentre region, and gradually becomes less pronounced towards the Laccadive Ridge.

Discussion and conclusions

We documented the magnitude and regional distribution of the depth anomaly over the 63–42 Ma oceanic crust of the Arabian Basin. The depth anomalies presented in this study are in line with the results obtained from different parts of the world ocean. One of the world's largest depth anomalies (named 'superswell' by McNutt and Fischer 1987) is reported in the South Pacific Ocean, where the depth anomaly (shallower than predicted) has a maximum amplitude of >1 km (McNutt and Sichoix 1996; Sichoix et al. 1998). Depth anomalies have also been reported from the Atlantic Ocean (Hayes 1988; Louden et al. 2004) and the Southeast Indian Ocean (Hayes 1988).

Several hypotheses have been forwarded to explain the origin of negative depth anomalies (swell). According to Sleep (1990), the regional domal uplift is a characteristic feature of the presence of mantle plumes. The change from vertical upwelling to horizontal flow along the base of the lithosphere induces an upward force on the plate (Menard 1973), causing a dome-shaped uplift around the centre of upwelling. Compilation of depth anomalies and hotspot locations of the world oceans also indicates a strong correlation between depth anomalies and occurrence of hotspots (Crough 1979). Mostly negative depth anomalies (swells) correlate with hotspots such as Iceland, the Azores, Cape Verde and Bermuda in the North Atlantic Ocean. The negative depth anomalies are often about a kilometre shallower than the neighbouring seafloor, and usually about 1,000 km wide.

Another possible contributor to oceanic depth anomalies is compositional buoyancy due to basalt extraction (Jordan 1979; Robinson 1988). Melting depletes fertile mantle in garnet, and raises the MgO/FeO ratio of the residuum which, as a consequence, becomes less dense (O'Hara 1975; Boyd and McCallister 1976; Oxburgh and Parmentier 1977), which therefore causes uplift. The thinning hypothesis (Detrick and Crough 1978) postulates that there is a

high mantle heat flux associated with each hotspot. Since the lithosphere is a thermal boundary layer, additional heat in the base of the lithosphere causes the lithospheric thickness to decrease. Because the lithosphere is colder and, therefore, denser than the asthenosphere, this thinning generates isostatic uplift and the formation of a topographic swell.

We propose that the negative depth anomaly (rise of oceanic basement) in the eastern part of the Arabian Basin is due to its proximity to the high thermal regime of the former Reunion hotspot. It would appear that vertical upwelling due to convection, followed by a lateral across-axis flow driven by excess near-field pressure by the hotspot, may have induced an upward force on the plate. Thereafter, the oceanic lithosphere started subsiding, and is presently relatively shallow, compared to the depth of the normal oceanic crust predicted by Stein and Stein (1992), even if the cause(s) of the uplift have ceased to operate in the region. It may be mentioned here that the Arabian and Eastern Somali basins evolved due to a complex pattern of spreading-ridge propagation between magnetic chrons 28n (~63 Ma) and 20n (~43 Ma; Dyment 1998; Chaubey et al. 1998, 2002). As a result, asymmetric crustal accretion occurred in the two basins over this whole period. Although the origin and change in direction of propagation of the palaeo-propagators in these basins are not well understood, a linkage between the former Reunion hotspot and the spreading-ridge propagation has been postulated in earlier studies (Dyment 1998; Chaubey et al. 1998). Royer et al. (2002) argued that the former Reunion hotspot may have generated a regional swell which was large enough to affect the bathymetry of the region, which would explain the spreading-ridge propagation 'downhill' along the bathymetry or gravity gradient (Morgan and Sandwell 1994). These views support the postulate that the nearby former Reunion hotspot influenced the evolution of the oceanic crust of the basins. We therefore postulate that the zone of negative depth anomalies documented in this study is caused by vertical upwelling due to convection, followed by a lateral across-axis flow facilitated by the Reunion hotspot. This is further supported by the spatial as well as temporal proximity of the Reunion hotspot to the early Tertiary seafloor-spreading regime in the eastern part of the Arabian Basin (Whitmarsh 1974; Morgan 1981; Shipboard Scientific Party 1988).

The zone of positive depth anomalies located in the western part of the Arabian Basin indicates excess subsidence of the oceanic crust relative to that predicted by thermal cooling and thickening of normal oceanic lithosphere. We surmise that the excess subsidence of the western part of the Arabian Basin is caused by the combination of isostatic adjustment due to

sediment loading and the relatively cold mantle, compared to the nearby eastern part of the basin affected by the intense thermal field of the former Reunion hotspot. The spreading-ridge segments, 'hotter' than normal, are likely to preserve their on and off-axis properties as long as the cause of the anomaly remains intact, because the hot anomaly is self-buoyant in an upwelling and diverging environment (Chiao and Wang 1999; Ito 2001). Lin et al. (2002) proposed that dynamic interaction between relatively cold mantle beneath spreading ridges and the ambient flow renders a transient nature to the subsidence of the seafloor.

Excess subsidence of oceanic crust can be caused by a number of other mechanisms, such as isostatic adjustment due to sediment loading, evacuation of magma chambers beneath the crust due to volcanism, and visco-elastic flexure of the underlying lithosphere due to convective currents. However, to establish the origin and actual cause of the positive depth anomaly observed in the western part of the Arabian Basin, additional data are required. The results of this study warrant further in-depth documentation and analysis of the depth anomaly in both the Arabian and Eastern Somali basins to understand the mechanisms responsible for it, in particular the interaction of the former Reunion hotspot with spreading ridges in early Tertiary times.

Acknowledgements

We are grateful to Dr. Satish Shetye, Director, National Institute of Oceanography, Goa, for encouragement, support and permission to publish this work. KKA thanks the Council of Scientific and Industrial Research, New Delhi, for financial assistance in the form of a Junior Research Fellowship. This work was carried out under the project DST/23(339)/SU/2002 of the Department of Science & Technology, New Delhi. We are thankful to Prof. Burg W. Flemming, Editor-in-Chief, Dr. Monique T. Delafontaine, Associate Editor and two anonymous reviewers, whose comments and suggestions have helped greatly to improve the manuscript. This is NIO contribution 4261.

References

Bhattacharji S, Chatterjee N, Wampler JM, Nayak PN, Deshmukh SS (1996) Indian intraplate and continental margin rifting, lithospheric extension, and mantle upwelling in Deccan flood basalt volcanism near the K/T boundary: evidence from mafic dike swarms. Geology 104:379–398

Bhattacharya GC, Chaubey AK, Murty GPS, Gopala Rao D, Scherbakov VS, Lygin VA, Philipenko AI, Bogomyagkov AP (1992) Marine magnetic anomalies in the northeastern Arabian Sea. In: Desai BN (ed) Oceanography of the Indian Ocean. Oxford IBH, New Delhi, pp 503–509

Bhattacharya GC, Chaubey AK, Murty GPS, Srinivas K, Sarma KVLNS, Subrahmanyam V, Krishna KS (1994) Evidence for seafloor spreading in the Laxmi Basin, northeastern Arabian Sea. Earth Planet Sci Lett 125:211–220

Boyd FR, McCallister RH (1976) Densities of sterile and fertile garnet peridotites. Geophys Res Lett 3:509–512

Cande SC, Kent DV (1995) Revised calibration of the geomagnetic polarity timescale for the Late Cretaceous and Cenozoic. J Geophys Res 100:6093–6095

Chaubey AK, Bhattacharya GC, Murty GPS, Desa M (1993) Spreading history of the Arabian Sea: some new constraints. Mar Geol 112:343–352

Chaubey AK, Bhattacharya GC, Rao DG (1995) Seafloor spreading magnetic anomalies in the southeastern Arabian Sea. Mar Geol 128:105–114

Chaubey AK, Bhattacharya GC, Murty GPS, Srinivas K, Ramprasad T, Gopala Rao D (1998) Early Tertiary seafloor spreading magnetic anomalies and paleo-propagators in the northern Arabian Sea. Earth Planet Sci Lett 154:41–52

Chaubey AK, Dyment J, Bhattacharya GC, Royer J-Y, Srinivas K, Yatheesh V (2002) Paleogene magnetic isochrons and palaeo-propagators in the Arabian and Eastern Somali basins, NW Indian Ocean. In: Clift PD, Kroon D, Gaedicke C, Craig J (eds) The tectonic and climatic evolution of the Arabian Sea region. Spec Publ Geol Soc Lond 195:71–85

Chiao LY, Wang CW (1999) Effect of near-ridge thermal anomalies on the subsidence of the oceanic lithosphere: constraints from a 2-D dynamic model. Geophys Res Lett 26:807–810

Courtillot V, Besse J, Vandamme D, Montigny R, Jaeger JJ, Cappetta H (1986) Deccan flood

basalts at the Cretaceous/Tertiary boundary? Earth Planet Sci Lett 80:361–374

Crough ST (1979) Hotspot epeirogeny. In: McGetchni TR, Merrill RB (eds) Plateau uplift: mode and mechanism. Tectonophysics 61:321–333

Crough ST (1983) The correction for sediment loading on the sea floor. J Geophys Res 88:6449–6454

Davis EE, Lister CRB (1974) Fundamentals of ridge crest topography. Earth Planet Sci Lett 21:405–413

Detrick RS, Crough ST (1978) Island subsidence, hotspots and lithospheric thinning. J Geophys Res 83:1236–1244

Dyment J (1998) Evolution of the Carlsberg Ridge between 60 and 45 Ma: ridge propagation, spreading asymmetry and the Deccan-Reunion hotspot. J Geophys Res 103:24,067–24,084

Hayes DE (1988) Age-depth relationships and depth anomalies in the Southeast Indian Ocean and South Atlantic Ocean. J Geophys Res 93:2,937–2,954

Hillier JK, Watts AB (2004) "Plate-like" subsidence of the East Pacific Rise-South Pacific super swell system. J Geophys Res109 B10102 DOI 10.1029/2004JB003041

Ito G (2001) Reykjanes 'V'-shaped ridges originating from a pulsing and dehydrating mantle plume. Nature 411:681–684

Jordan TH (1979) Mineralogies, densities and seismic velocities of garnet lherzolites and their geophysical implications. In: Boyd FR, Meyer HOA (eds) The mantle sample: inclusions in kimberlites and other volcanics. American Geophysical Union, Washington, DC, pp 1–14

Lin SC, Chiao LY, Kuo BY (2002) Dynamic interaction of cold anomalies with the mid-ocean ridge flow field and its implications for the Australian-Antarctic Discordance. Earth Planet Sci Lett 203:925–935

Louden KE, Tucholke BE, Oakey GN (2004) Regional anomalies of sediment thickness, basement depth and isostatic crustal thickness in the North Atlantic Ocean. Earth Planet Sci Lett 224:193–211

Malod JA, Droz L, Kemal BM, Patriat P (1997) Early spreading and continental to oceanic basement transition beneath the Indus deep-sea fan: northeastern Arabian Sea. Mar Geol 141:221–235

McKenzie D, Sclater JG (1971) The evolution of the Indian Ocean since the Late Cretaceous. Geophys J R Astron Soc 25:437–528

McKenzie D, Watts A, Parson B, Roufosse M (1980) Planform of mantle convection beneath the Pacific Ocean. Nature 288:442–446

McNutt MK, Fischer KM (1987) The south Pacific superswell. In: Keating BH, Fryer P, Batiza R, Boehlert GW (eds) Seamounts, islands and atolls. American Geophysical Union, Washington, DC, Geophys Monogr Ser 43:25–34

McNutt M, Sichoix L (1996) Modal depths from shipboard bathymetry: there is a south Pacific superswell. Geophys Res Lett 23:3397–4000

Menard HW (1969) Elevation and subsidence of oceanic crust. Earth Planet Sci Lett 6:275–284

Menard HW (1973) Depth anomalies and bobbing motion of drifting islands. J Geophys Res 78:5128–5137

Mercuriev S, Patriat P, Sochevanova N (1995) Evolution de la dorsale de Carlsberg: évidence pour une phase d'expansion très lente entre 40 et 25 Ma (A18 à A7). Oceanol Acta 19:1–13

Miles PR, Roest WR (1993) Earliest sea-floor spreading magnetic anomalies in the north Arabian Sea and the ocean-continent transition. Geophys J Int 115:1025–1031

Morgan WJ (1981) Hotspot tracks and the opening of the Atlantic and Indian Oceans. In:

Emiliani C (ed) The Sea, vol 7. The oceanic lithosphere. Wiley, New York, pp 443-487

Morgan JP, Sandwell DT (1994) Systematics of ridge propagation south of 30°S. Earth Planet Sci Lett 121:245–258

Nafe JE, Drake CL (1963) Physical properties of marine sediments. In: Hill MN (ed) The Sea, vol 3. Ideas and observations on progress in the study of the sea. Wiley, New York, pp 794–815

Naini BR (1980) A geological and geophysical study of the continental margin of western India and the adjoining Arabian Sea including the Indus Cone. PhD Thesis, Columbia University, New York

Naini BR, Talwani M (1983) Structural framework and the evolutionary history of the continental margin of western India. In: Watkins JS, Drake CL (eds) Studies in continental margin geology. Am Assoc Petrol Geol Mem 34:167–191

Norton IO, Sclater JG (1979) A model for the evolution of the Indian Ocean and the breakup of the Gondwanaland. J Geophys Res 84:6803–6830

O'Hara MJ (1975) Is there an Icelandic mantle plume? Nature 253:708–710

Oxburgh ER, Parmentier EM (1977) Compositional and density stratification in oceanic lithosphere – causes and consequences. J Geol Soc Lond 133:343–355

Parsons B, Sclater JG (1977) An analysis of the variation of ocean floor bathymetry and heat flow with age. J Geophys Res 82:803–827

Patriat P, Achache J (1984) India-Eurasia collision chronology has implications for crustal shortening and driving mechanism of plates. Nature 311:615–621

Robinson EM (1988) The topographic and gravitational expression of density anomalies due to melt extraction in the uppermost oceanic mantle. Earth Planet Sci Lett 90:221–228

Royer J-Y, Chaubey AK, Dyment J, Bhattacharya GC, Srinivas K, Yatheesh V, Ramprasad T (2002) Palaeogene plate tectonic evolution of the Arabian and Eastern Somali basins. In: Clift PD, Kroon D, Gaedicke C, Craig J (eds) The tectonic and climatic evolution of the Arabian Sea region. Spec Publ Geol Soc Lond 195:7–23

Sclater JG, Francheteau J (1970) The implications of terrestrial heat flow observations on current tectonic and geochemical models of the crust and upper mantle of the earth. Geophys J R Astron Soc 20:509–542

Shipboard Scientific Party (1988) Site 715. In: Backman J, Duncan RA and 24 others (eds) Proceedings Ocean Drilling Program, College Station, TX, pp 917–946

Sichoix L, Bonneville A, McNutt MK (1998) The seafloor swells and superswell in French Polynesia. J Geophys Res 103:27,123–27,133

Sleep NH (1990) Hotspots and mantle plumes: some phenomenology. J Geophys Res 95:6715–6736

Stein CA, Abbott DH (1991) Heatflow constraints on the south Pacific superswell. J Geophys Res 96:16083–16099

Stein CA, Stein S (1992) A model for the global variation in oceanic depth and heat flow with lithospheric age. Nature 359:123–129

Vandamme D, Courtillot V, Besse J, Montigny R (1991) Paleomagnetism and age determination of the Deccan Traps (India): results of a Nagpur-Bombay traverse and review of earlier work. Rev Geophys 29:159–190

Wessel P, Smith WHF (1995) New version of the generic mapping tools released. EOS Trans Am Geophys Union 76:1–329

Whitmarsh RB (1974) Some aspects of plate tectonics in the Arabian Sea. Init Rep DSDP 23:527–535

Whitmarsh RB, Weser OE and 10 others (1974) Sites 219, 220 and 221. Init Rep DSDP 23:35–210

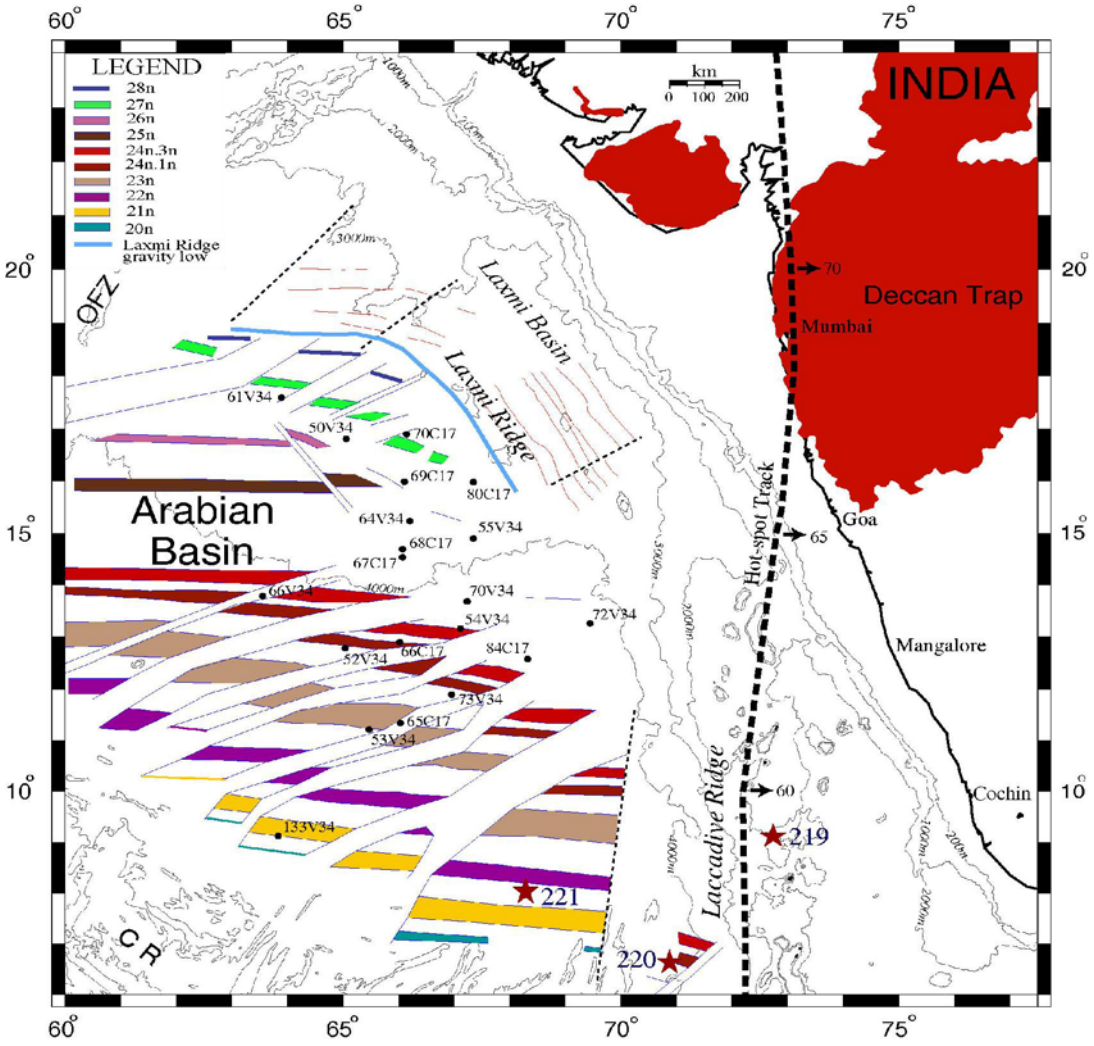

Fig. 1 Generalized tectonic map of the Arabian Basin and adjacent region, showing magnetic lineations, pseudofaults (*thin blue lines*), fracture zones (*dashed lines*) and main structural features (Chaubey et al. 2002). Locations of seismic refraction stations used in this study are shown with *solid annotated dots* (Naini and Talwani 1983); DSDP drill sites are shown by *solid stars* (Whitmarsh et al. 1974); *solid thick dashed line* represents the computer-modelled Reunion hotspot track; *numbers* along the hotspot track are predicted ages in Ma (Shipboard Scientific Party 1988); also shown are magnetic lineations in the Laxmi Basin (*thin red lines*; Bhattacharya et al. 1994; Malod et al. 1997). *CR* Carlsberg Ridge, *OFZ* Owen Fracture Zone

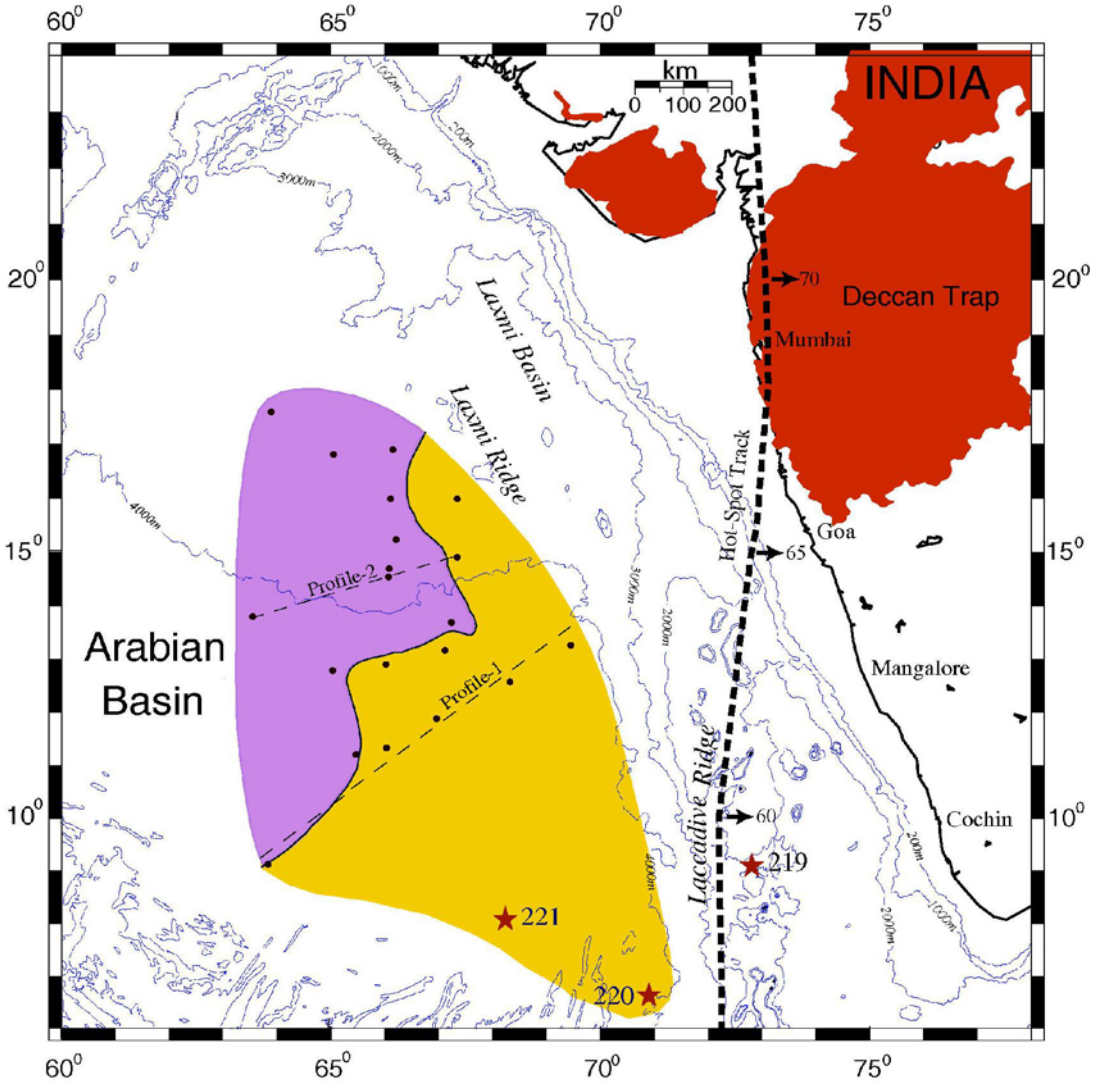

Fig. 2 Map showing distribution of basement depth anomalies in the Arabian Basin. The anomalies vary from 501 to –905 m (Table 1) and display two distinct patterns – a zone of negative anomalies (*yellow-shaded*), followed by a zone of positive anomalies (*violet-shaded*). Positive anomalies represent deeper basement depth than predicted, whereas negative anomalies indicate shallower basement depth than predicted. Locations of refraction stations and the computer-modelled Reunion hotspot track are shown as *solid dots* and *thick dashed line* respectively; *numbers* along the hotspot track are predicted ages in Ma (Shipboard Scientific Party 1988). The depth anomaly curves shown in Fig. 3 have been prepared on the basis of traverses *1* and *2*

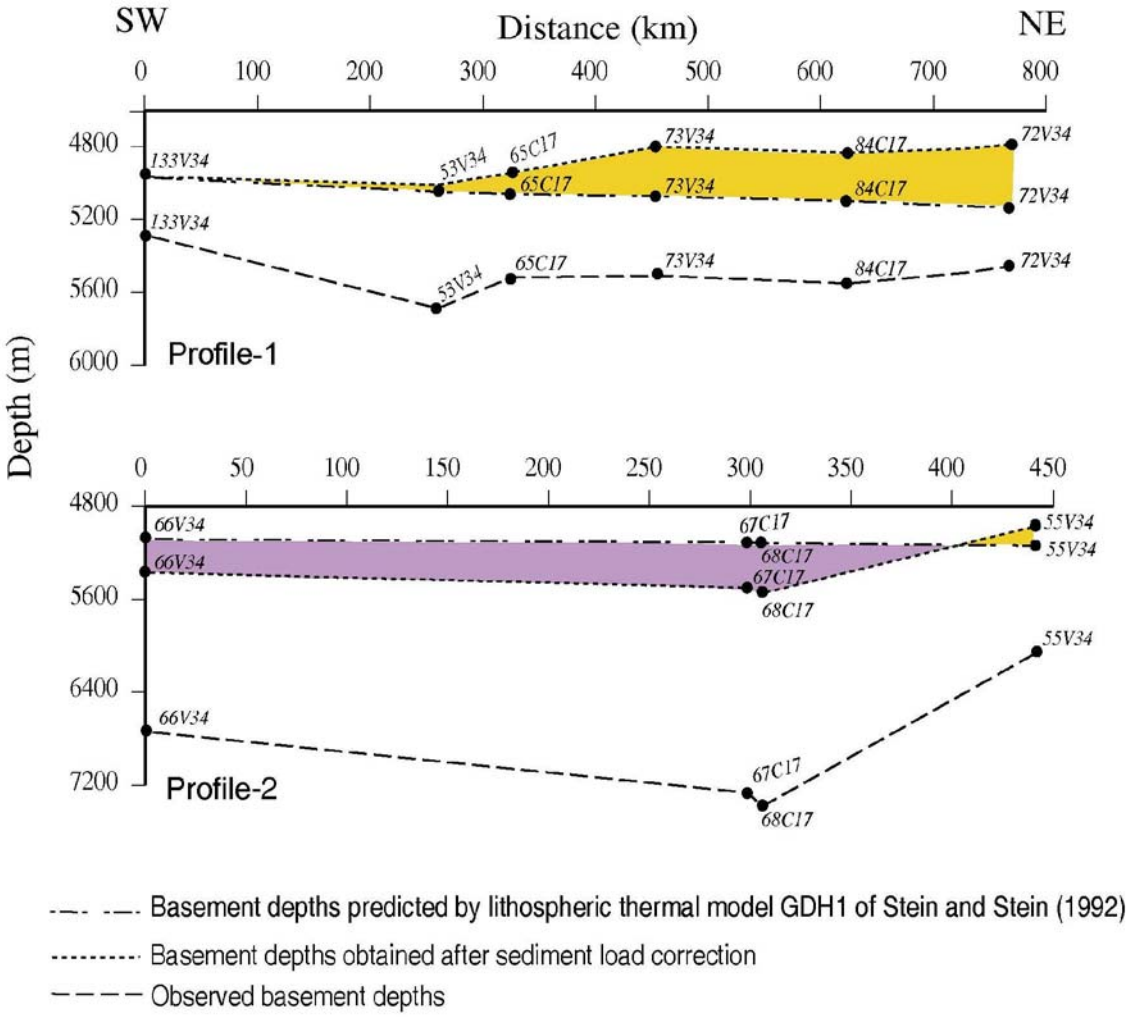

Fig. 3 Two northeast–southwest profiles (cf. Fig. 2) across the Arabian Basin, showing (i) observed basement depths, (ii) basement depths obtained after sediment load correction and (iii) basement depths predicted by lithospheric thermal model GDH1 of Stein and Stein (1992)

Table 1 Basement depth anomalies computed at refraction stations in the Arabian Basin

Refraction stations	Age	Water depth	Sediment thickness	Present basement depth	Predicted basement depth	Average seismic velocity	Sediment density	Sediment load correction	Sediment-corrected basement depth	Basement depth anomaly
	(Ma)	(m)	(m)	(m)	(m)	(km/s)	(g/cm^3)	(m)	(m)	(m)
61V34	60.303	3,505	3,640	7,145	5,188	2.72	2.15	1,838	5,343	154
70C17	61.436	3,580	3,770	7,350	5,203	2.71	2.15	1,910	5,490	287
50V34	59.570	3,538	3,580	7,118	5,179	2.68	2.14	1,829	5,367	189
80C17	61.410	3,720	970	4,690	5,202	2.06	1.95	577	4,297	–905
69C17	59.223	3,730	3,070	6,800	5,174	2.60	2.14	1,574	5,304	130
64V34	55.885	3,703	3,380	7,083	5,128	2.64	2.14	1,726	5,429	301
55V34	56.439	3,769	2,290	6,059	5,136	2.38	2.07	1,237	5,006	–130
68C17	54.916	3,840	3,550	7,390	5,114	2.73	2.17	1,775	5,615	501
67C17	54.639	3,780	3,490	7,270	5,110	2.62	2.14	1,785	5,565	455
66V34	52.903	3,992	2,750	6,742	5,083	2.60	2.12	1,425	5,417	334
70V34	54.270	3,814	2,660	6,474	5,104	2.56	2.11	1,393	5,207	103
54V34	53.347	3,983	1,860	5,843	5,090	2.41	2.07	1,006	4,989	–101
66C17	52.663	4,030	1,950	5,980	5,079	2.56	2.11	1,021	5,051	–28
52V34	52.290	3,996	2,050	6,046	5,073	2.36	2.06	1,123	5,119	46
72V34	56.255	4,017	1,440	5,457	5,133	2.29	2.05	794	4,811	–322

Refraction stations	Age	Water depth	Sediment thickness	Present basement depth	Predicted basement depth	Average seismic velocity	Sediment density	Sediment load correction	Sediment-corrected basement depth	Basement depth anomaly
	(Ma)	(m)	(m)	(m)	(m)	(km/s)	(g/cm^3)	(m)	(m)	(m)
84C17	53.855	4,120	1,430	5,550	5,098	2.54	2.11	752	4,873	–225
73V34	52.197	4,128	1,380	5,508	5,072	2.73	2.16	696	4,824	–247
65C17	51.380	4,220	1,300	5,520	5,058	2.18	2.00	744	4,964	–94
53V34	50.780	4,198	1,490	5,688	5,048	2.15	1.99	863	5,061	13
133V34	46.260	4,361	925	5,286	4,968	1.75	1.82	603	4,964	–4
DSDP221	48.440	4,650	261	4,911	5,008	1.65	1.75	178	4,828	–180
DSDP220	52.198	4,036	330	4,366	5,072	1.60	1.70	232	4,268	–803